DETERMINATION OF FORMATION PROPERTIES IN CASED BOREHOLES USING FULL WAVEFORM ACOUSTIC LOGS

by

Kenneth M. Tubman, C.H. Cheng, and M. Nafi Toksöz

Earth Resources Laboratory
Department of Earth, Atmospheric, and Planetary Sciences
Massachusetts Institute of Technology
Cambridge, MA 02139

ABSTRACT

Wave propagation in bonded and unbonded cased boreholes is examined through the calculation of synthetic full waveform acoustic logs. The models consist of a central fluid borehole surrounded by a number of fluid and solid annuli. Waveforms calculated for a variety of formation and cement parameters demonstrate that the first arrivals observed on full waveform acoustic logs in well bonded cased holes are those of the formation and not the casing. Waves refracted along the casing are generally too small to be observed. The presence of the steel and cement can make the determination of formation velocities more difficult than in an open hole. The formation body wave arrivals are decreased substantially if the cement velocities are near or greater than the formation velocities. A fluid layer between the steel and the cement essentially frees the pipe from the cement. The steel arrival then becomes a large, ringing signal which obscures the formation arrival. The presence of this layer is a more important factor than its thickness in causing such behavior. If the fluid layer is between the cement and the formation, the cement can damp out the ringing of the pipe. If a thick cement layer is bonded to the pipe and the fluid layer is thin, the casing arrival is small and the formation arrivals are discernible. A thinner cement layer results in the observation of a body wave that has a velocity that is an average of the steel and cement velocities.

INTRODUCTION

Previous studies have examined wave propagation in cased boreholes. Most have been for bond logging applications though, and so concentrated on determining cement parameters and bonding conditions (Walker, 1968; Riddle, 1962; Pardue *et al.*, 1963; Brown *et al.*, 1970). Tubman *et al.* (1984) made the assumption that the steel was completely bonded to the cement which was in turn completely bonded to the formation. Chang and Everhart, (1983) accounted for other than perfect bonding by allowing discontinuities in the axial displacement at the steel-cement interface and requiring the axial stress to go to zero at this boundary. Their formulation did not include any additional fluid layers.

In this study we examine full waveform acoustic logs in boreholes with unbonded in addition to well-bonded casing. The situation of unbonded casing and cement is modeled through the inclusion of fluid layers intermixed with the

solid layers of the steel, cement, and formation.

SYNTHETIC MICROSEISMOGRAMS

Synthetic full waveform acoustic logs are generated for cased hole geometries. The borehole geometry is modeled as a number of homogeneous, isotropic annuli surrounding a central fluid cylinder. The number of annuli is arbitrary, as well as whether each is a solid or fluid. The only restrictions are that the central cylinder is fluid and the outer, infinite formation is solid. Attenuation is included in the calculations through the use of complex layer velocities. The synthetic waveforms are calculated using the method of discrete wavenumber integration (Cheng and Toksöz, 1981; Tubman *et al.*, 1984) and contain all body and guided waves. The source (the same as that used by Tubman *et al.*, 1984) is centered at 13 kHz. Layers of steel and cement are within an infinite formation in the model of a well bonded cased hole. A fluid layer is placed between the steel and the cement to model poor pipe-cement bonding, and between the cement and the formation to model poor cement-formation bonding. More details of the method are given in Tubman *et al.* (1984) and Cole (1983). The parameters used in the generation of the synthetic microseismograms are given with each figure.

Well Bonded Casing and Cement

Figure 1 shows the microseismogram for a model consisting of layers of steel, cement, and formation surrounding the central fluid cylinder. This is the geometry used to represent a well bonded cased hole. There are fairly clear body and guided wave arrivals. The velocities of these waves are determined by finding the moveout of the arrivals with increasing source-receiver separation. The body wave velocities determined in this manner correspond to the formation velocities and not those of the casing or cement. This is demonstrated further by modifying individual parameters of the model. The formation velocities are lowered in the model used in the calculation of the microseismogram of Figure 2. All other parameters remain unchanged. The compressional and shear velocities are lowered so as to maintain a constant V_p / V_s ratio for the two formations. If the observed arrivals were from the casing, and not from the formation, little difference would be expected between the waveforms. It is clear, though, that the velocities determined from the microseismograms in Figure 2 are different from those in Figure 1. The velocities measured from Figure 2 again correspond to the formation velocities. It is interesting to note that, while the body wave arrival times have changed significantly, the Stoneley wave arrival time has changed only slightly. This indicates that the dominant influence on the Stoneley wave (aside from that of the borehole fluid) is from the steel and the cement, with the formation having very little effect. The thickness of the cement layer is important in controlling the nature of the Stoneley wave. The formation has more influence if the cement layer is very thin or non-existent.

The presence of the steel and the cement can make determination of the formation velocities more difficult though. This is illustrated in the microseismograms shown in Figures 3 and 4. The cement velocities used in the model for Figure 3 have been raised so that they are now close to those of the

formation. As can be seen from the figure, the amplitudes of the body waves have decreased considerably relative to the previous cases. This is because the contrast between the steel and cement is less so there is less energy directed back to the receiver. The pseudo-Rayleigh mode is also reduced in amplitude. The faster cement pushes the pseudo-Rayleigh dispersion curves to higher frequency, but since the center frequency of the source remains constant, there is a smaller frequency range over which these waves are excited.

The model used in the calculation of Figure 4 has a formation with velocities which are comparable to those of the steel casing. The P wave arrival is clear and can be determined to be the formation velocity. In this case, there is a large amount of ringing between the P wave arrival and the Stoneley wave arrival. This ringing has a wavelength which is about four times the thickness of the cement layer. It appears that a low velocity layer of cement trapped between the higher velocity steel and formation sets up some resonance phenomenon that is dominating this portion of the signal. It is difficult to identify any distinct arrivals between the first P wave and the Stoneley wave. Thus, it is clear that in well-bonded case holes, one can generally determine the formation velocities. The identification of the formation arrivals, particularly the S wave or pseudo-Rayleigh wave arrival, depends on the relative velocities of the cement and the formation.

No Steel-Cement Bond, Good Cement-Formation Bond

Unfortunately, bonding conditions in boreholes do not always match the perfect bonding situation modeled above. In general there are two locations where the bonding can be less than ideal: at the steel-cement interface, and at the cement-formation interface. The first situation is examined here by inserting a layer of fluid between the steel casing and the cement. This is the free pipe situation. The synthetic microseismograms calculated for this case are shown in Figures 5, 6 and 7. In Figure 5, the fluid layer between the steel and the cement is taken to be 0.5 inches thick. As shown in the figure, there is a large, distinct arrival at the beginning of the signal. The velocity of this arrival corresponds to the plate velocity of the steel, not the velocity of the formation. With the pipe not well bonded to the cement, the casing arrival has a large amplitude and long duration. The formation P wave arrival is completely overpowered by this signal. The above observation is consistent with field data (Walker, 1968; Grosmangin *et al.*, 1961).

A situation that is less well understood is when the thickness of the intermediate fluid layer becomes very small. The thin layer of fluid is commonly referred to as a microannulus. The model of Chang and Everhart (1983) is the limit of this situation with the thickness of the fluid layer equal to zero. In Figures 6 and 7 we present synthetic microseismograms in two different formations each with a microannulus of thickness 0.001 inches surrounding the casing. Even with such a thin fluid layer, the first arrival in Figure 6 is a ringing signal from the casing. Changing the formation properties has little effect on the nature of the waveform. The velocities (both compressional and shear) of the formation in Figure 7 are less than those in Figure 6. The remainder of the model parameters are the same in both figures. There are no changes in the first arrivals in these cases as there were in the well bonded situations.

Good Steel-Cement Bond, No Cement-Formation Bond

Another common occurrence in cased holes is good steel-cement bonding but poor cement-formation bonding. In Figures 8 — 12 we present synthetic microseismograms modeling this situation. The intermediate fluid layer is between the cement and the formation so the steel casing is now clad with a layer of cement. In Figure 8 the thickness of the fluid layer is 0.0625 inches and the thickness of the cement layer is 1.6875 inches. The cement is sufficiently thick here to damp out the ringing of the casing observed in the free pipe situation. The arrival from the casing is very small. The velocity of the first obvious arrival corresponds to the P wave velocity of the formation. The formation S wave arrival is also clear. To check that these are indeed the formation arrivals, the casing parameters are held constant and the formation velocities are modified. The resulting microseismograms are shown in Figure 9. It is clear from this figure that the arrival times and velocities of the body waves have changed as the formation velocities change. Velocities determined from this figure confirm that the observed arrivals are from the formation and not from the casing.

If the cement layer is thinner it will not be able to damp out the casing arrivals effectively. Figure 10 shows the synthetic microseismograms from a model with a cement layer thickness of 0.5 inches and a fluid layer thickness of 1.25 inches. The amplitude of the first arrival has increased relative to the previous cases of thicker cement. The duration of this portion of the waveform has also increased substantially. The formation shear and pseudo-Rayleigh wave arrivals are now much more difficult to identify due to overlapping with the ringing of the earlier arrival. Changing the formation parameters has little effect on the shape and velocity of this first arrival. This is seen in Figure 11, which was calculated with the same geometry but with a slower formation. The first wave packets on waveforms in both Figures 10 and 11 are virtually identical. The velocity of this first arrival is determined to be between the plate velocity of the steel and the velocity of the cement. In Figure 12 the velocities of the cement have be increased so that they are now comparable to the formation velocities. This relationship between the cement and formation velocities in the well-bonded cased hole resulted in significantly reduced amplitudes of the first arrival (Figure 3). Here, the amplitudes and shape of the first arrival are almost unchanged. The velocity has increased slightly though, due to the faster cement. The amplitude and velocity of this wave increase with decreasing thickness of the cement layer. A similar amplitude variation of the casing signal with cement thickness was observed by Walker (1968) using data from test wells.

CONCLUSIONS

Three types of bonding situations commonly encountered in cased holes are studied through the calculation of synthetic full waveform acoustic log microseismograms.

In the case of good bonding between steel and cement and between cement and formation, the layers of steel and cement generally have only a small influence on the formation body wave arrivals. It is possible for these layers to make the determination of formation velocities more difficult than in an open

hole. If the cement velocities are comparable to those of the formation the amplitude of the formation arrivals can be significantly reduced. The steel and cement, along with the fluid, exert the dominant influence on the Stonely wave.

A fluid layer between the steel and cement effectively frees the steel casing. The result is that the casing arrival becomes larger in amplitude and longer in duration. The casing signal in this situation dominates the formation P wave signal. There is little change in the nature of the waveform as the thickness of the fluid layer is changed. It is the the presence of this layer, not its thickness, that is the most important factor in the behavior of the casing arrival.

When there is poor bonding between the cement and the formation but good bonding between the steel and the cement, the situation is more complicated. It may be possible to discern the formation body wave arrivals even in the presence of a fluid layer between the cement and the formation. If the fluid layer is thin and there is a large amount of cement bonded to the pipe, the cement will act to damp out the ringing of the pipe, making the formation arrivals clear. If the cement layer is sufficiently thin, it will ring along with the steel casing. The first arrival in this situation will be from the combination of the steel and the cement and will have a velocity intermediate to their velocities.

ACKNOWLEDGEMENTS

This work was supported by the Full Waveform Acoustic Logging Consortium at M.I.T. Kenneth Tubman was partially supported by a Phillips Petroleum Company Fellowship.

REFERENCES

Brown, H.D., Grijalva, V.E., and L.L. Raymer, 1970, New developments in sonic wave train display and analysis in cased holes: Trans. S.P.W.L.A., paper F.

Chang, S.K. and Everhart, A.H., 1983, A study of sonic logging in a cased borehole: J. Pet. Tech., v.35., p.1745-1750.

Cheng, C.H. and Toksöz M.N., 1981, Elastic wave propagation in a fluid-filled borehole and synthetic acoustic logs: Geophysics; v.46, p.1042-1053.

Cole, S.P., 1983, Guided wave dispersion in a borehole containing multiple fluid layers, B.S. Thesis, Department of Physics, Massachusetts Institute of Technology, Cambridge, MA.

Grosmangin, M., Kokesh, F.P., and Majani, P., 1961, A sonic method for analyzing the quality of cementation of borehole casings: J. Pet. Tech., p.165-171.

Pardue, G.H., Morris, R.L., Gollwitzer, L.H., and Moran, J.H.,1963, Cement bond log - A study of cement and casing variables: J. Pet. Tech. p.545-555.

Riddle, G.A., 1962, Acoustic wave propagation in bonded and unbonded oil well casing: S.P.E. paper number 454.

Tubman, K.M., Cheng, C.H., and Toksöz, M.N., 1984, Synthetic full waveform acoustic logs in cased boreholes: Geophysics, in press.

Walker, T., 1968, A full-wave display of acoustic signal in cased holes: J. Pet. Tech., p.818-824.

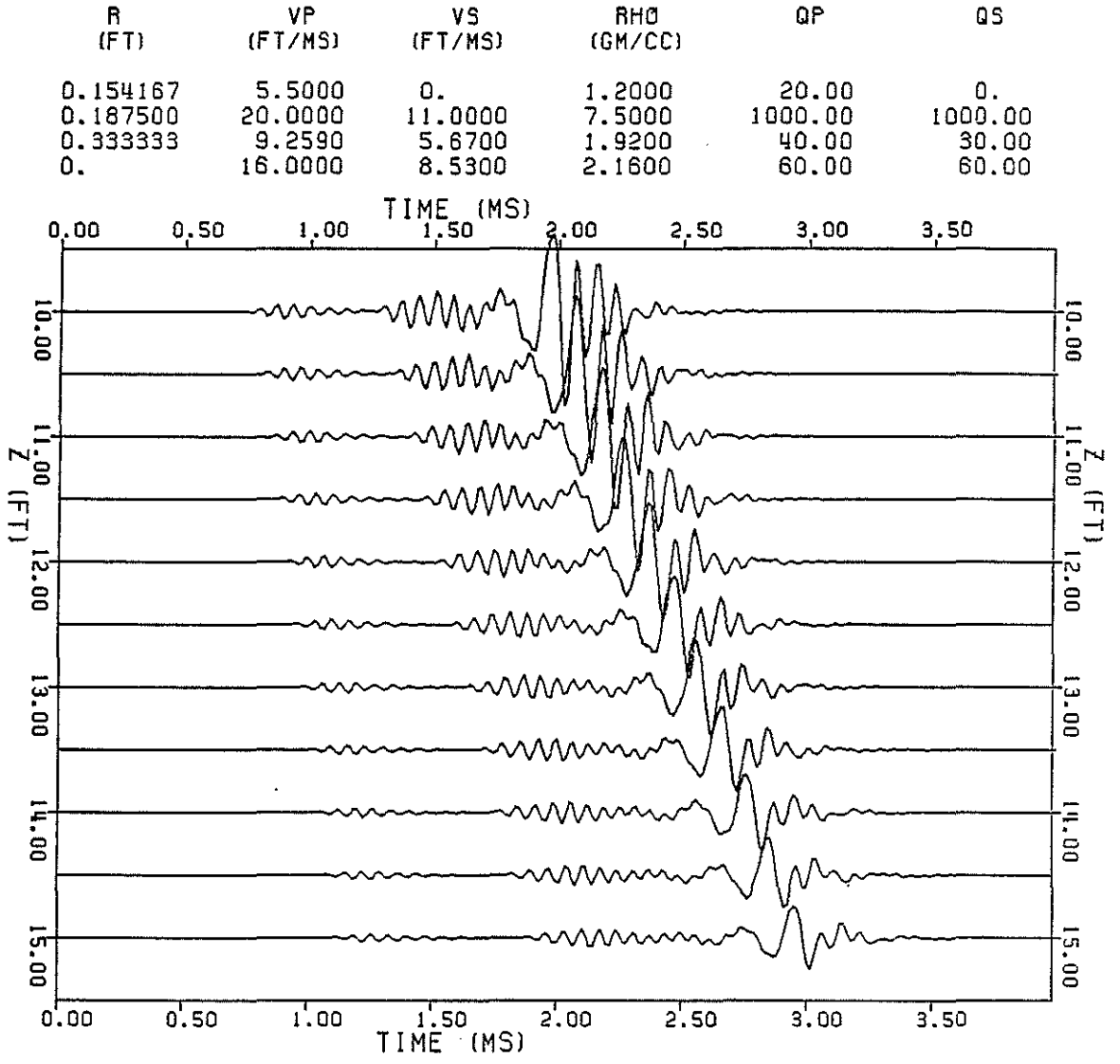

FIG. 1. Synthetic microseismograms in a well bonded cased hole for offsets varying from 10 ft. to 15. ft at .5 ft intervals. R is the outer radius of the layer; V_p and V_s the compressional and shear velocities; ρ the density; and Q_p and Q_s the compressional and shear quality factors. The bottom layer (R = 0.) is the infinite formation.

R (FT)	VP (FT/MS)	VS (FT/MS)	RHO (GM/CC)	QP	QS
0.154167	5.5000	0.	1.2000	20.00	0.
0.187500	20.0000	11.0000	7.5000	1000.00	1000.00
0.333333	9.2590	5.6700	1.9200	40.00	30.00
0.	13.1200	7.0000	2.1600	60.00	60.00

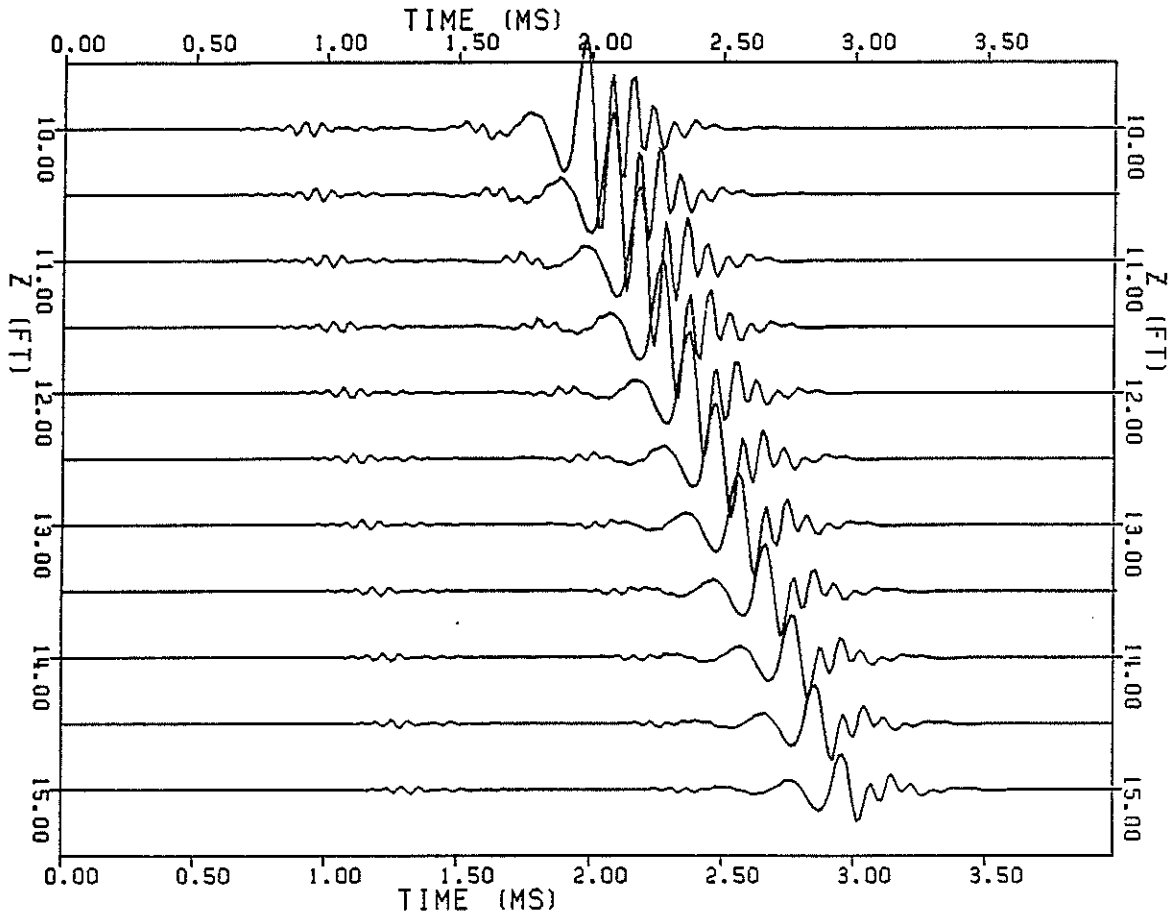

FIG. 2. Same as Figure 1. with a slower formation.

R (FT)	VP (FT/MS)	VS (FT/MS)	RHO (GM/CC)	QP	QS
0.154167	5.5000	0.	1.2000	20.00	0.
0.187500	20.0000	11.0000	7.5000	1000.00	1000.00
0.333333	13.5000	8.3000	1.9200	40.00	30.00
0.	16.0000	8.5300	2.1600	60.00	60.00

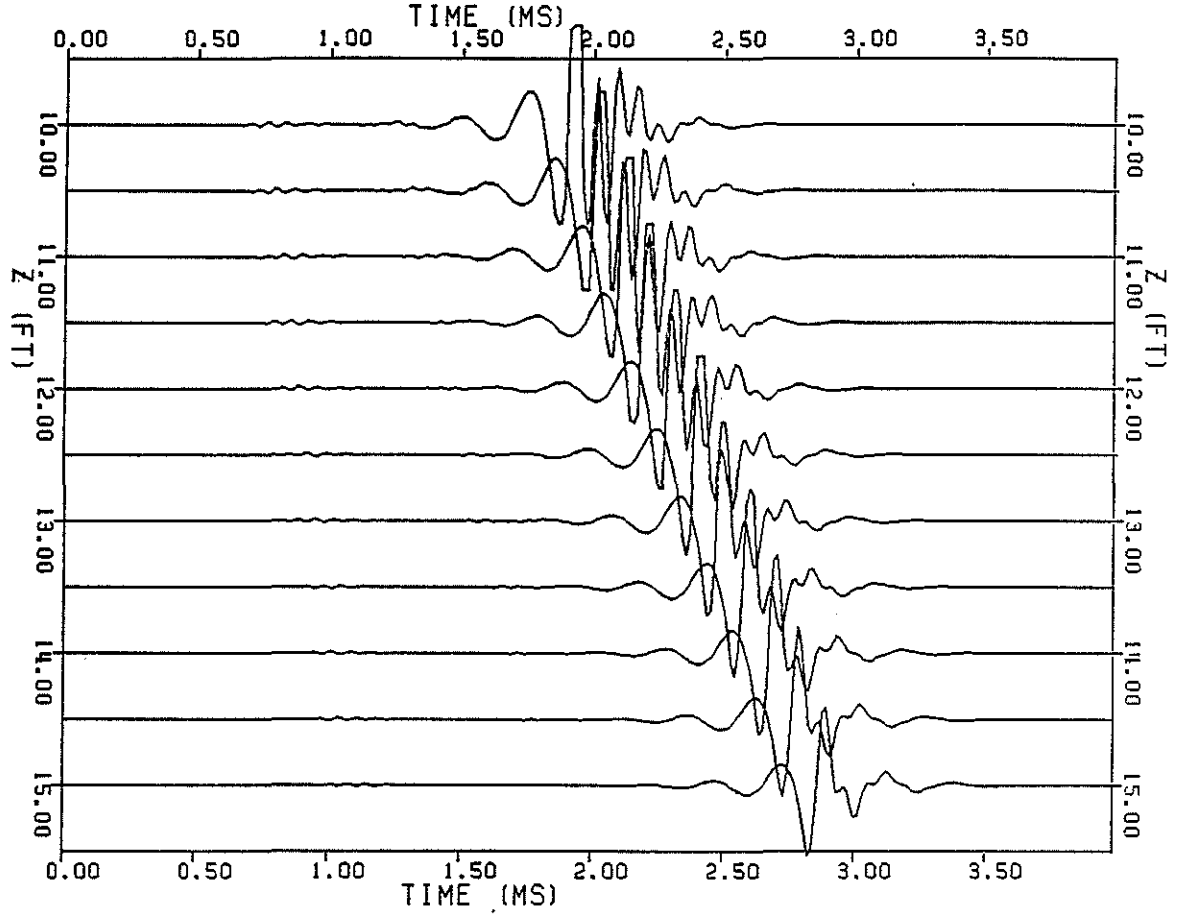

FIG. 3. Microseismograms for a model with cement velocities close to the formation velocities. The amplitude scale (gain) is twice that of the other figures.

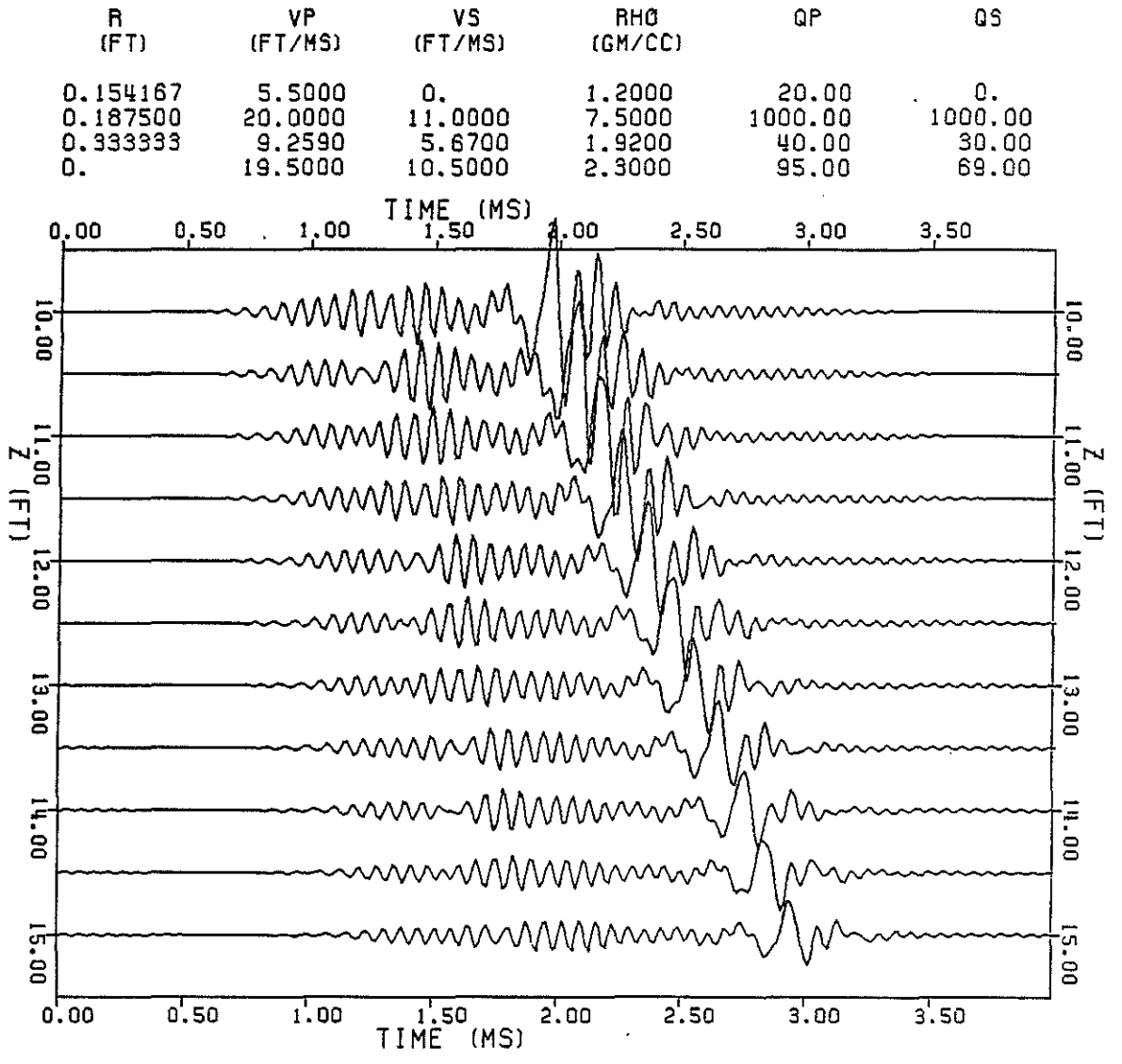

FIG. 4. Microseismograms for a model with formation velocities comparable to the casing velocities.

R (FT)	VP (FT/MS)	VS (FT/MS)	RHO (GM/CC)	QP	QS
0.154167	5.5000	0.	1.2000	20.00	0.
0.187500	20.0000	11.0000	7.5000	1000.00	1000.00
0.229167	5.5000	0.	1.2000	20.00	0.
0.333333	9.2590	5.6700	1.9200	40.00	30.00
0.	13.1200	7.0000	2.1600	60.00	60.00

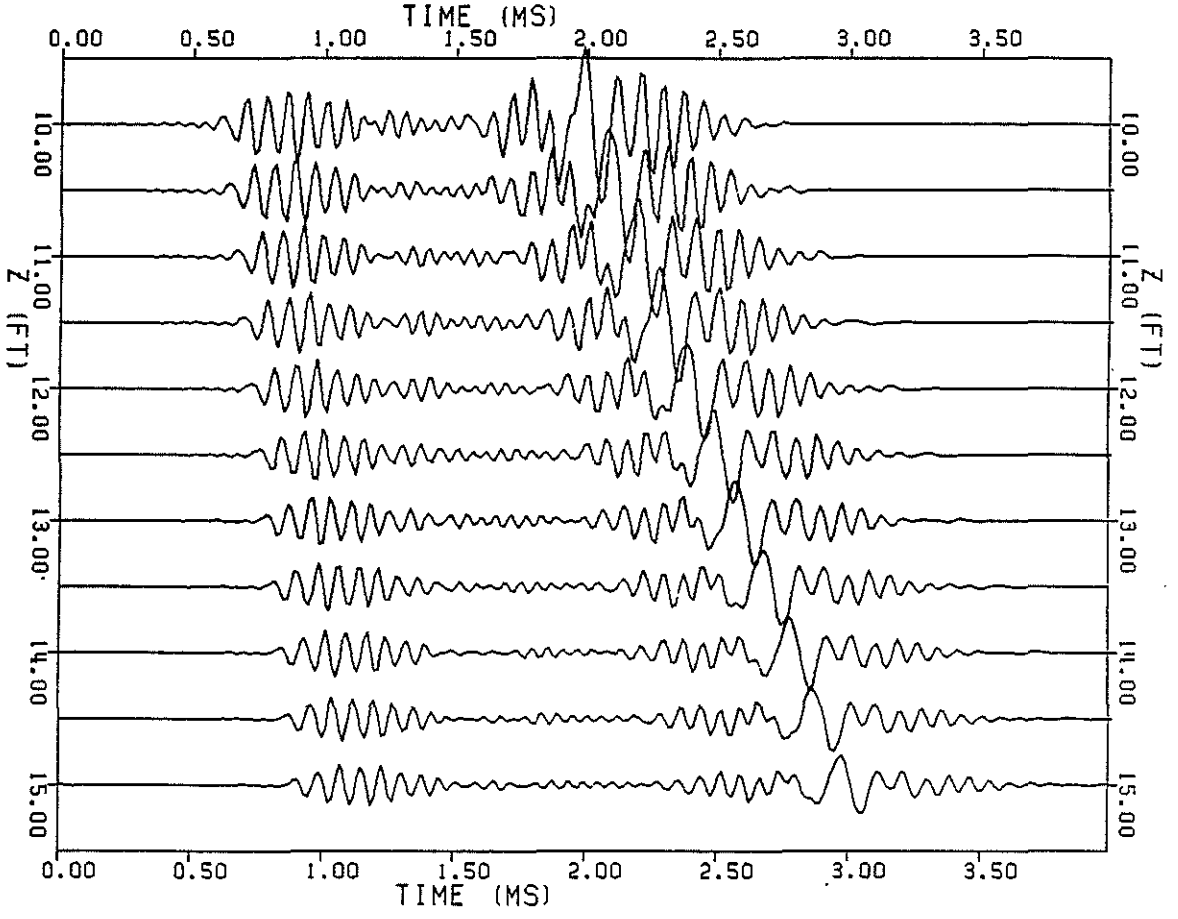

FIG. 5. Microseismograms for the free pipe situation. There is a .5 inch fluid layer between the steel and the cement.

R (FT)	VP (FT/MS)	VS (FT/MS)	RHO (GM/CC)	QP	QS
0.154167	5.5000	0.	1.2000	20.00	0.
0.187500	20.0000	11.0000	7.5000	1000.00	1000.00
0.187583	5.5000	0.	1.2000	20.00	0.
0.333333	9.2590	5.6700	1.9200	40.00	30.00
0.	16.0000	8.5300	2.1600	60.00	60.00

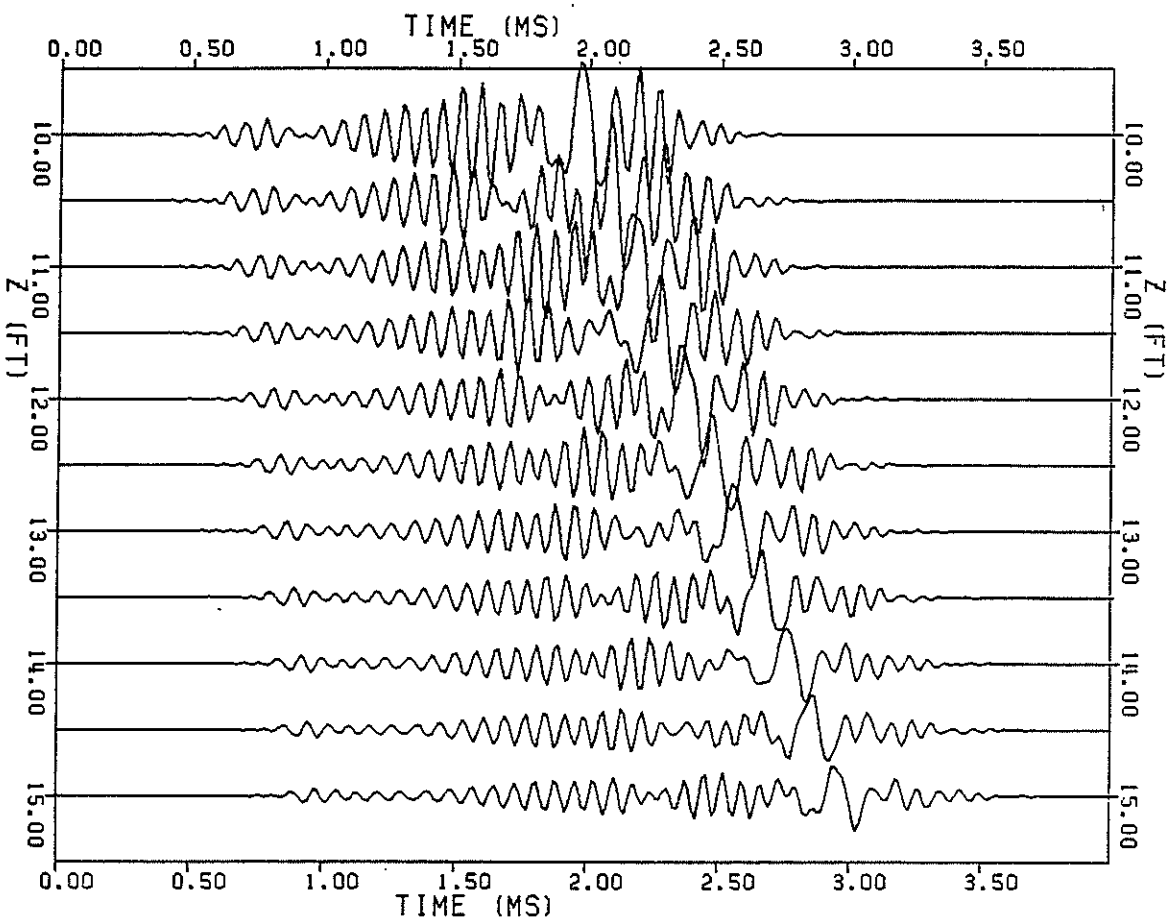

FIG. 6. Microseismograms for a model of a microannulus. The fluid layer between the pipe and cement is .001 inches thick.

R (FT)	VP (FT/MS)	VS (FT/MS)	RHO (GM/CC)	QP	QS
0.154167	5.5000	0.	1.2000	20.00	0.
0.187500	20.0000	11.0000	7.5000	1000.00	1000.00
0.187583	5.5000	0.	1.2000	20.00	0.
0.333333	9.2590	5.6700	1.9200	40.00	30.00
0.	13.1200	7.0000	2.1600	60.00	60.00

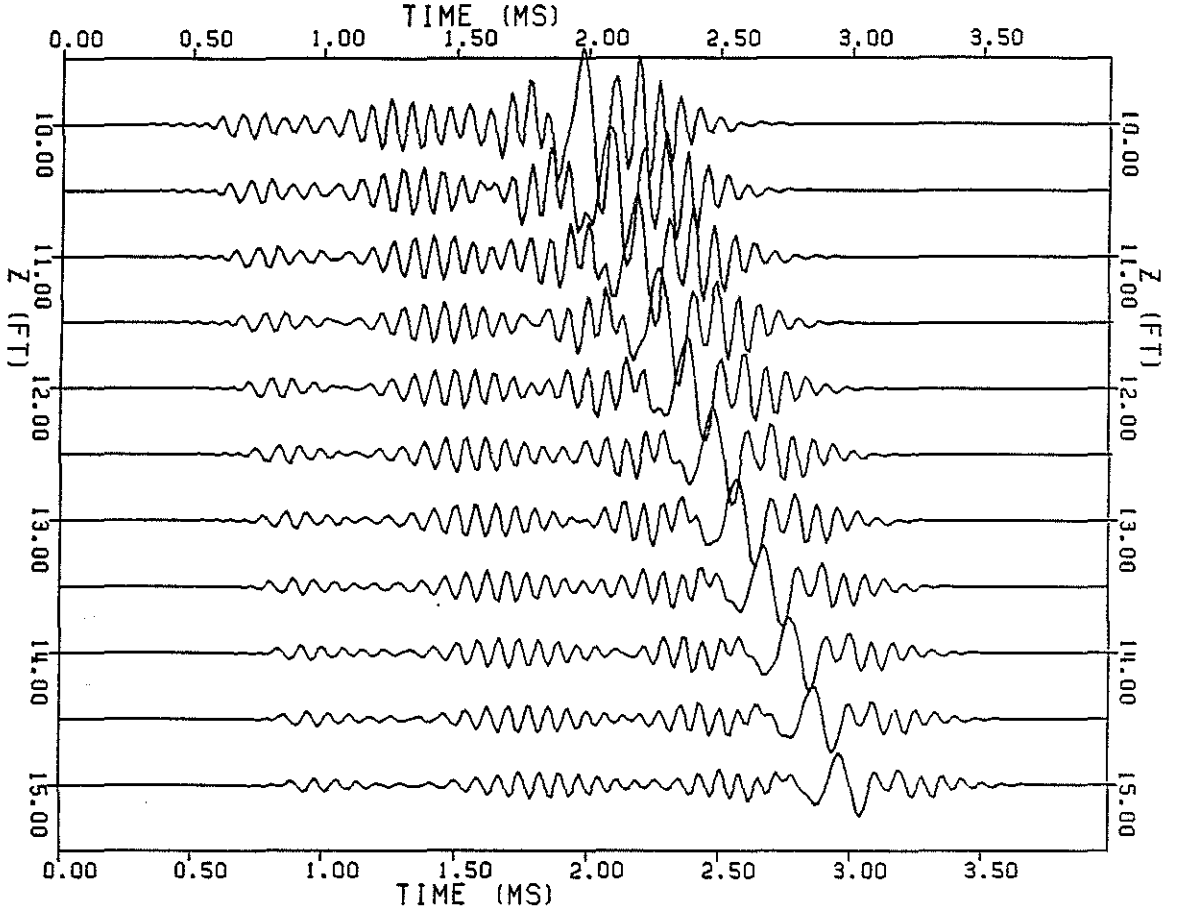

FIG. 7. Same as Figure 6 with lower formation velocities.

R (FT)	VP (FT/MS)	VS (FT/MS)	RHO (GM/CC)	QP	QS
0.154167	5.5000	0.	1.2000	20.00	0.
0.187500	20.0000	11.0000	7.5000	1000.00	1000.00
0.328125	9.2590	5.6700	1.9200	40.00	30.00
0.333333	5.5000	0.	1.2000	20.00	0.
0.	16.0000	8.5300	2.1600	60.00	60.00

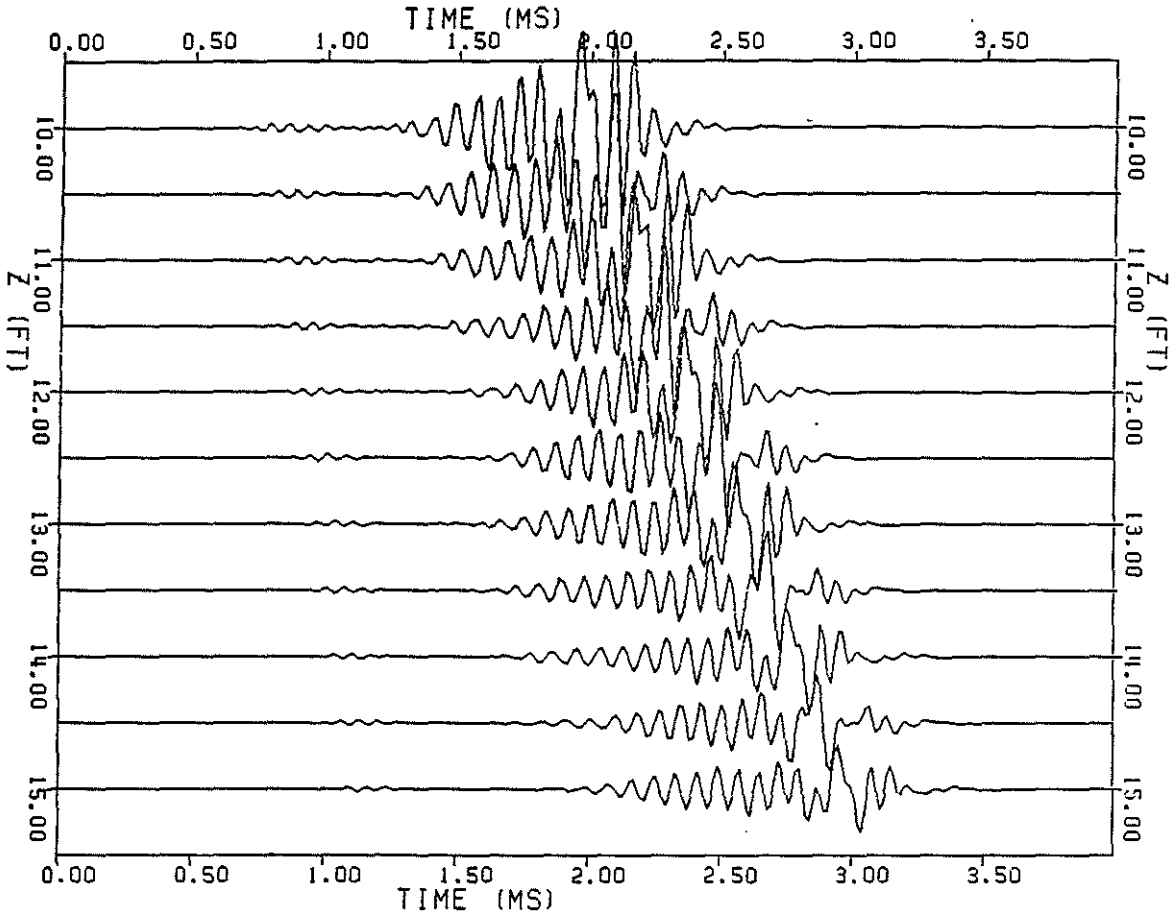

FIG. 8. Microseismograms for a model with good steel-cement bonding but no cement-formation bonding. There is a thick cement layer bonded to the pipe.

R (FT)	VP (FT/MS)	VS (FT/MS)	RHO (GM/CC)	QP	QS
0.154167	5.5000	0.	1.2000	20.00	0.
0.187500	20.0000	11.0000	7.5000	1000.00	1000.00
0.328125	9.2590	5.6700	1.9200	40.00	30.00
0.333333	5.5000	0.	1.2000	20.00	0.
0.	13.1200	7.0000	2.1600	60.00	60.00

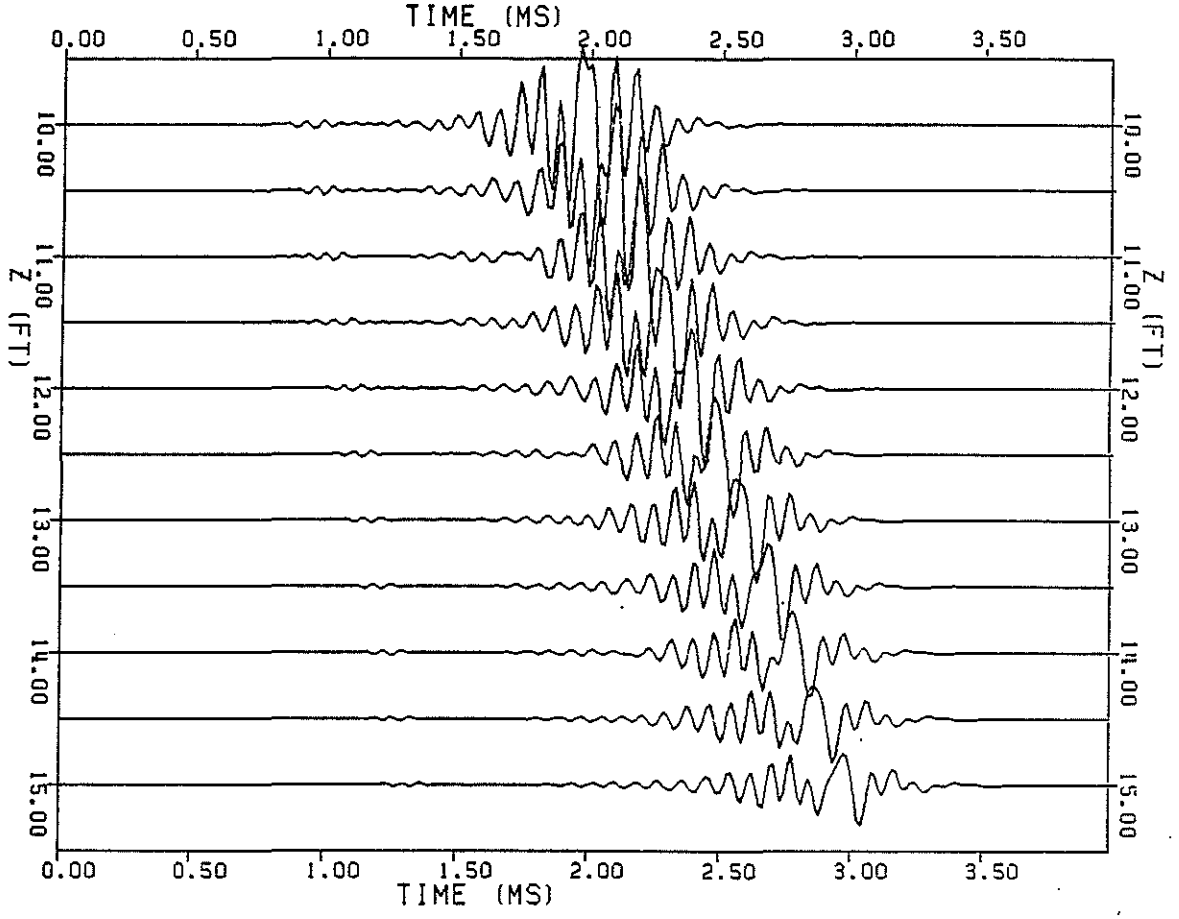

FIG. 9. Same as Figure 8 with lower formation velocities.

R (FT)	VP (FT/MS)	VS (FT/MS)	RHO (GM/CC)	QP	QS
0.154167	5.5000	0.	1.2000	20.00	0.
0.187500	20.0000	11.0000	7.5000	1000.00	1000.00
0.229167	9.2590	5.6700	1.9200	40.00	30.00
0.333333	5.5000	0.	1.2000	20.00	0.
0.	16.0000	8.5300	2.1600	60.00	60.00

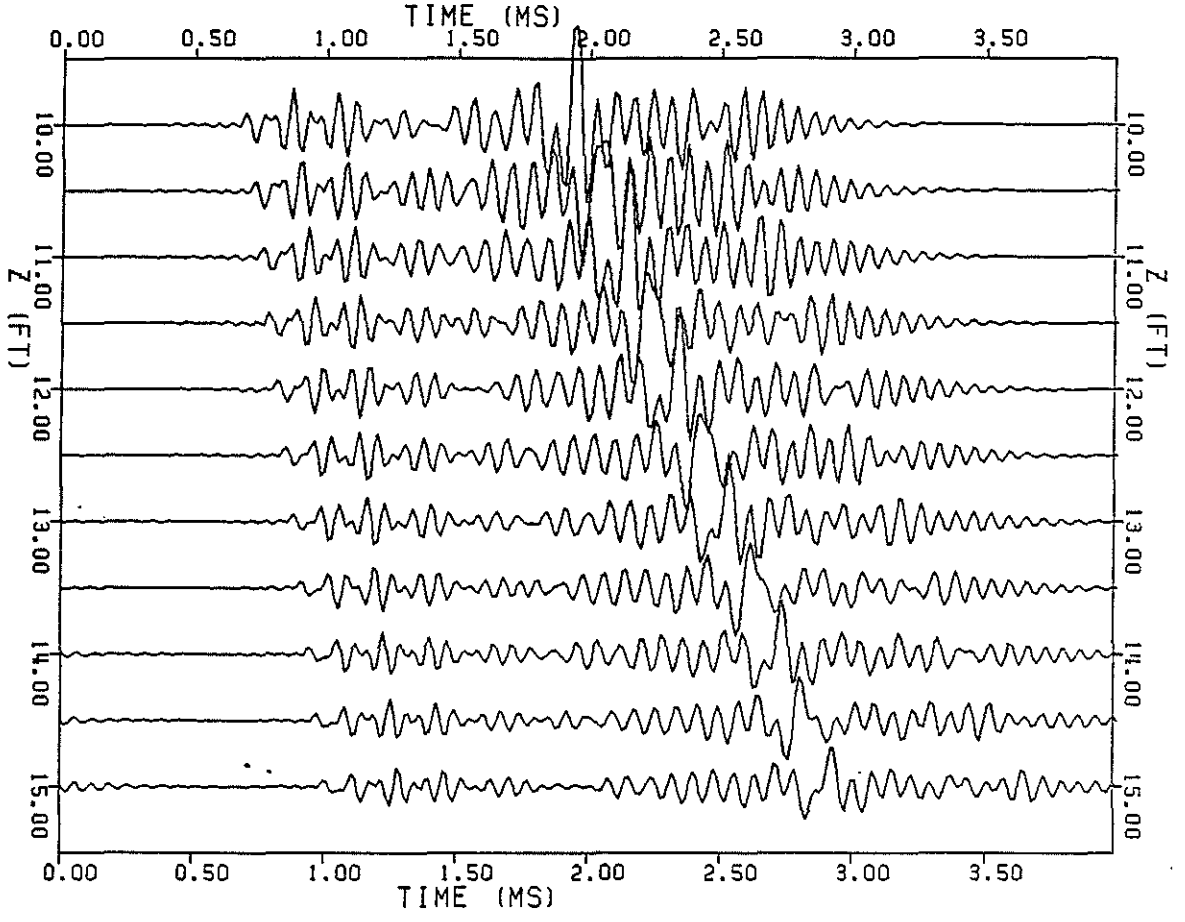

FIG. 10. Microseismograms for a model with a thin layer of cement bonded to the pipe and a thick fluid layer between the cement and the formation.

R (FT)	VP (FT/MS)	VS (FT/MS)	RHO (GM/CC)	QP	QS
0.154167	5.5000	0.	1.2000	20.00	0.
0.187500	20.0000	11.0000	7.5000	1000.00	1000.00
0.229167	9.2590	5.6700	1.9200	40.00	30.00
0.333333	5.5000	0.	1.2000	20.00	0.
0.	13.1200	7.0000	2.1600	60.00	60.00

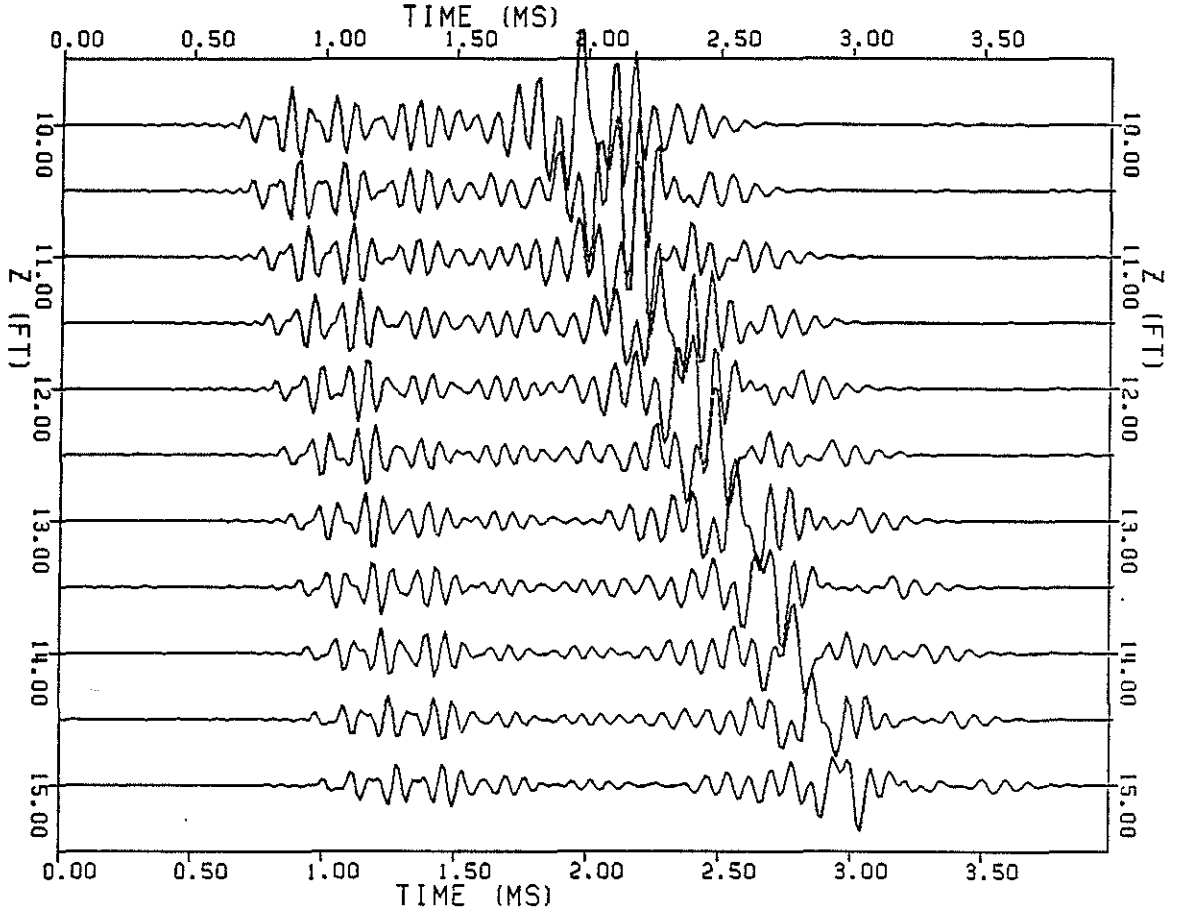

FIG. 11. Same as Figure 10 with lower formation velocities.

R (FT)	VP (FT/MS)	VS (FT/MS)	RHO (GM/CC)	QP	QS
0.154167	5.5000	0.	1.2000	20.00	0.
0.187500	20.0000	11.0000	7.5000	1000.00	1000.00
0.229167	13.5000	8.3000	1.9200	40.00	30.00
0.333333	5.5000	0.	1.2000	20.00	0.
0.	16.0000	8.5300	2.1600	60.00	60.00

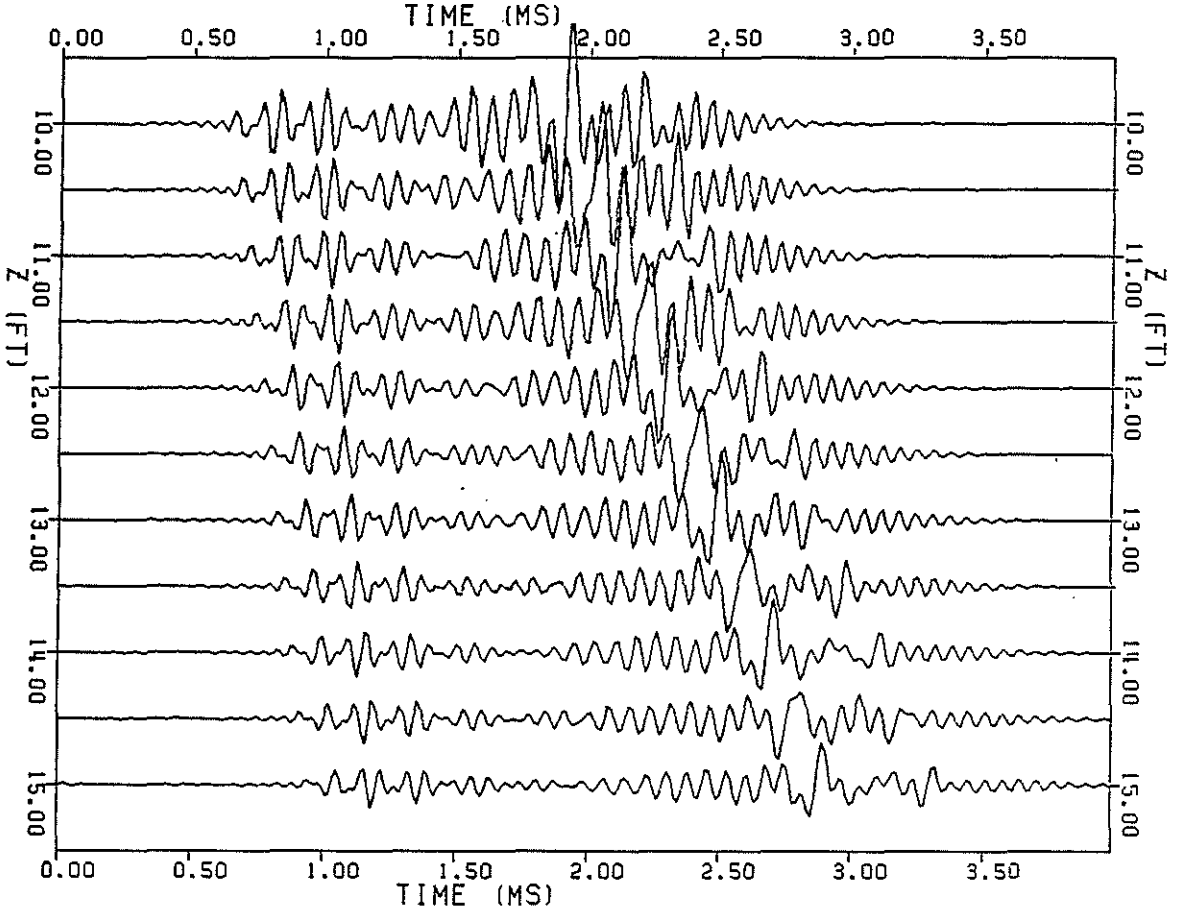

FIG. 12. Same as Figure 10 with higher cement velocities.